Int. J. Electrochem. Sci., 12 **(2017)** 2754 – 2762, doi: 10.20964/2017.04.25

International Journal of
ELECTROCHEMICAL
SCIENCE
www.electrochemsci.org

Dynamic Behavior of Silicon-Based Electrodes at Open Circuit Conditions

V. V. Emets, T. L. Kulova, and A. M. Skundin[*]

Frumkin Institute of Physical Chemistry and Electrochemistry, 31 Leninskii ave., 119071 Moscow, Russia
[*]E-mail: askundin@mail.ru

Received: 11 January 2017 / *Accepted:* 22 February 2017 / *Published:* 12 March 2017

The behavior of thin-film multi-layered silicon-based electrode during storage at open circuit conditions was studied for the first time by electrochemical impedance spectroscopy (EIS). The active part of electrode consisted of alternating layers of slightly oxidized silicon and Si-Al-O composite. It is found that self-discharge occurs during o.c.p. storage, and self-discharge current varies in chaotic manner. This phenomenon was explained by a dynamical character of SEI formation and destruction. The equivalent circuit comprising small inductance, ohmic resistance, and three parallel combinations of resistances and CPEs was proposed. The certain components of the equivalent circuit also undergo non-monotonous changes during the storage. This fact confirms dynamic character of SEI formation which manifests itself not only at the cycling but at open circuit conditions as well.

Keywords: electrochemical impedance spectroscopy; silicon composites; processes at electrode aging.

1. INTRODUCTION

Silicon and silicon-based composites are considered now as rather promising materials for negative electrodes of lithium-ion batteries. The main advantage of such materials is high theoretical capacity (4200 mAh g^{-1} for fully lithiated state $Li_{22}Si_5$ or 3580 mAh g^{-1} for the most popular $Li_{15}Si_4$). At the same time, silicon undergoes huge volume changes upon lithium insertion at the charge and lithium extraction at the discharge. This phenomenon results in strong mechanical strains, and finally in poor cyclability. That is why a lot of various sophisticated versions of silicon-based electrodes were proposed including nanomaterials and composites. There is abundant literature on electrochemical behavior and various properties of such electrodes, but authors failed to find information about their storage behavior. Meanwhile, shelf-life as well as cycle-life are rather important parameters of

batteries. It is worth noting that certain attention was paid to storage behavior of lithium-ion batteries with other types of negative electrodes. Early studies (see, e.g. [1–5]) were devoted to aging of Generation I of lithium-ion batteries, containing carbon (graphite) negative electrodes and positive electrodes based on $LiCoO_2$. It was found that it is precisely negative electrode that responsible for aging degradation of lithium-ion battery as whole. Later, some works on storage of batteries with positive electrodes based on lithiated nickel oxide [6], lithium iron phosphate [7], and NMC ($Li_{1.05}(Mn_{1/3}Co_{1/3}Ni_{1/3})_{0.95}O_2$)) [8–12] have appeared. Finally, the studies of aging of separate electrodes must be mentioned, including negative graphite electrodes [13–16], and positive electrodes based on $LiNi_yCo_{1-y}$ O_2 [17] and $LiCoO_2$ [18]. The mechanism of self-discharge of electrodes made from lithiated silicon was studied in [19] with static NMR measurements. The authors of [20] reported about binder impact upon degradation of electrodes based on SiO. The present work studies aging behavior of thin-film multi-layered negative electrodes consisting from alternating layers of Si-O and Si-O-Al. To the best of our knowledge, it is the first study of aging of silicon based electrodes. Thin-film multi-layered silicon-based electrodes are known to have much better cycleability than plain silicon ones [21–26]. That is why the present study has deal with these very electrodes.

2. EXPERIMENTAL

2.1. Electrodes fabrication

Thin-film multi-layered electrodes were prepared by magnetron sputtering with using simultaneously two targets, specifically, silicon and aluminum ones. The detailed description of the electrode manufacturing can be found elsewhere [27, 28]. The titanium foil with thickness 15 μm was used as a substrate. Both sides of this foil were treated with diluted mixture of sulfuric and hydrofluoric acids before the sputtering. The power of magnetron discharge was maintained at 420–480 W for silicon target and 200–210 W for aluminum one. The temperature of sputtering was 70 °C. Argon and oxygen were used as working gases. A silicon composite in the form of four-layer structure was deposited onto both sides of the foil. The first and the third layers with thickness ca. 0.2 μm, counting from substrate, were enriched with aluminum and the second and the fourth layers with thickness ca. 0.7 μm contained less aluminum. For lacking aluminum, the aluminum target was turned off. Si-Al alloy layers contained 36 wt % Al. Total oxygen content in the active layers was about 7 wt %. Although a system “silicon-oxygen” is the subject of a lot of studies, it is unknown in which form the oxygen exists in the composite, and this topic is out of scope of the paper. The fracture cross-section of Si-O-Al composite can be found in Fig. 1 of Ref. [28].

2.2. Electrochemical measurements

Electrochemical measurements were carried out in sealed cell of flat-parallel design. The cell contained one two-side working electrode, two lithium counter electrodes connected in parallel and placed opposite every side of the working electrode, and one lithium reference electrode. 1 M $LiPF_6$ in

ethylene carbonate - diethylcarbonate - dimethylcarbonate (1:1:1) mixture was used as an electrolyte. The cell was assembled in glove box with humidity about 10 ppm. We used non-woven polypropylene separator. The electrolyte humidity was less than 20 ppm. Preliminary galvanostatic cycling was performed with computerized cycler of Buster Co. (St. Petersburg, Russia). Potential limits of cycling were 0.01–2.0 V vs. lithium reference electrode. There were 5 charge-discharge cycles before the storage experiment. The last discharge run was finished after dissolution of small part of intercalated lithium. Then the cell was stored at open circuit conditions at room temperature for 72 days. Initial lithiation level was estimated with due account the initial value of open circuit potential (see below). Periodically open circuit potential (o.c.p.) was measured, and electrochemical impedance spectra (EIS) were registered in the frequency range from 10^{-2} to 10^{5} Hz. EIS measurements were carried out with using of the Solartron 1255 frequency response analyzer and the Solartron 1286 electrochemical interface. The amplitude of the applied voltage was 0.01 V. Impedance diagrams were fitted with the software Zplot®, from Scribner Associates.

3. RESULTS AND DISCUSSION

Open circuit potential of the electrode under study was close to 0.28 V at the very beginning of the experiment, that corresponded to partially lithiated state. Storage of the cell at open circuit conditions accompanied by shift of o.c.p. in positive direction (Fig. 1).

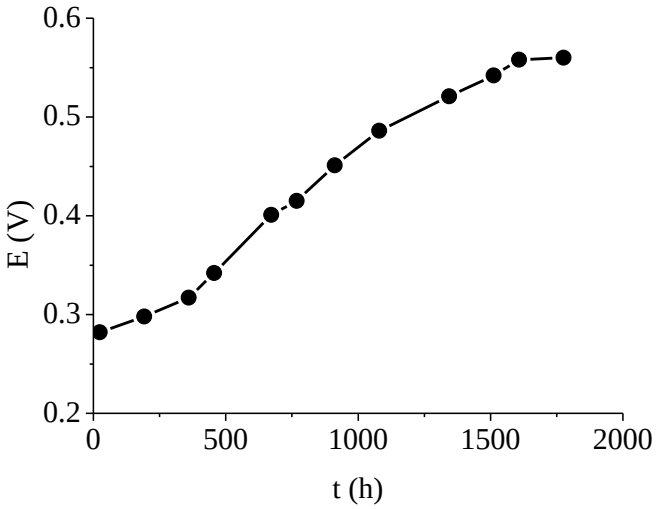

Figure 1. Variation of o.c.p. in the course of cell storage after 5 charge-discharge cycles

This shift of o.c.p. points to occurrence of anodic process of lithium leaching and some conjugated cathodic process of an electrolyte reduction. (The probability of anodic Al dissolution cannot be ruled out also. Current efficiencies of both anodic reactions remain un-known, but more likely than not, lithium is leached much faster than aluminum). The comparison of data of Fig. 1 with

dependence of o.c.p. on lithium content gives a possibility to estimate the rate of lithium leaching, i.e., corrosion current or self-discharge. We used anodic discharge curve taken at rather low current as "quasi-equilibrium" correlation between lithium content and o.c.p. This discharge curve is shown in Fig. 2. Of course, it is greatly desirable to have true equilibrium correlation between lithium concentration in silicon composite under study, and equilibrium potential. True equilibrium conditions are known to demand infinite time for measurement. It is known also, that a discharge curve registered with rather low C-rate is better approximation to equilibrium than corresponding charge curve. That is why, the data of Fig. 2 were used as almost equilibrium dependence of potential on lithium concentration.

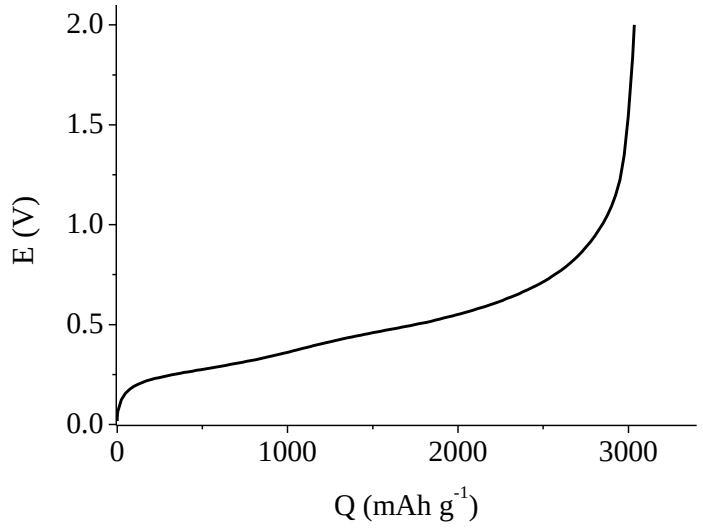

Figure 2. "Quasi-equilibrium" discharge curve registered at C/20.

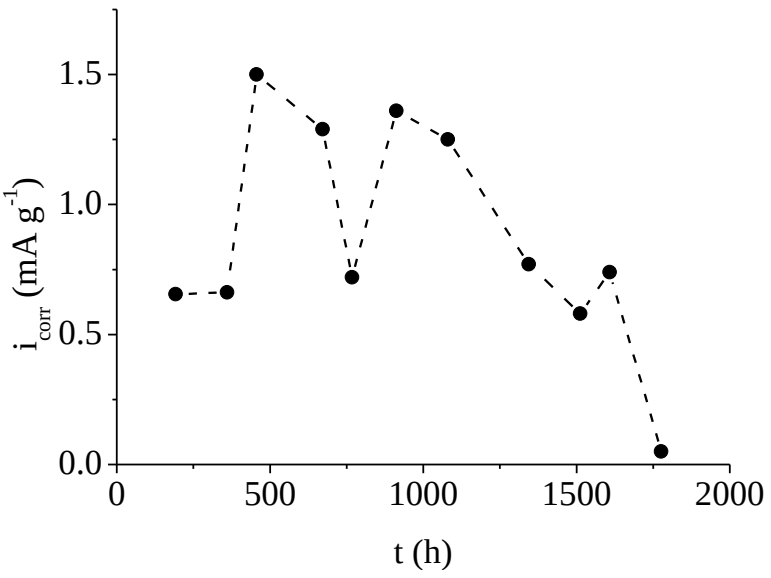

Figure 3. Corrosion current variation in the course of storage

Simple calculations show that the corrosion current was about 1 mA g^{-1} (order of magnitude), and this value on the whole corresponds to the electrode capacity and storage duration. Indeed, it is seen in Fig. 1 that after 24 hours the open circuit potential was equal to 0.282 V, and after 1776 hours it shifted up to 0.560 V. Fig. 2 shows that o.c.p. 0.560 V corresponds to extraction of 2040 mAh g^{-1}, whereas 0.282 V corresponds to 541 mAh g^{-1}. Therefore, total corrosion 2040 – 541 = 1499 mAh g^{-1} had place for 1776 – 24 = 1752 hours. So, average corrosion current was 1499 mAh g^{-1} : 1752 h = 0.855 ≈ 1 mA g^{-1}. It is important that corrosion current randomly varies in course of time (Fig. 3). The "instant" values of corrosion current were calculated with using Fig. 1 "point-to-point" as i = ΔQ/Δt, where ΔQ is a charge passed from one point to the following point, and Δt is corresponding time. It is interesting to compare the rate of self-discharge found in this work with values reported in the literature for other negative electrodes. According to [14], total self-discharge of fully lithiated graphite electrode occurred for 700 hours, that corresponds to average corrosion current about 0.5 mA g^{-1}.

Fig. 4 shows impedance diagrams (Nyquist plots) for various storage time, Fig. 4a referring to whole frequencies range, 4b referring to frequencies more than 0.1 Hz (for more detailed image).

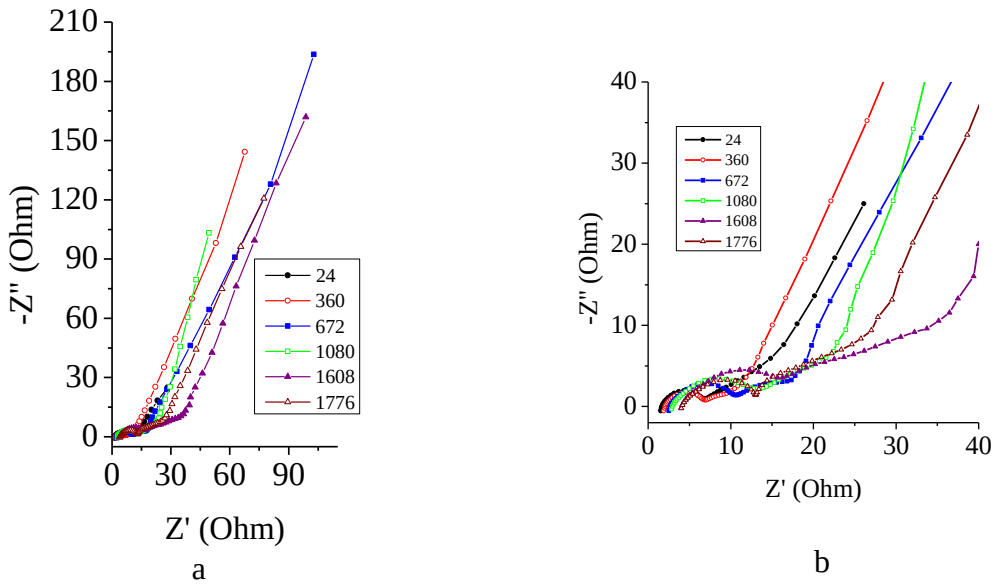

Figure 4. Nyquist plots for various storage time. Legends: storage time, hours. (a) – in the whole frequencies range 10^{-2} to 10^{5} Hz, (b) – in the frequencies range 10^{-1} to 10^{5} Hz

It is worth noting that the shape of spectra at Fig. 4 on the whole coincides with spectra for other silicon-based electrodes documented in the literature, see, e.g. [29–41], although all these spectra differ in details. Low-frequency part of spectra in Fig. 4 could be presented by straight lines with slope close to 2.5. Close values of slopes of spectra low-frequencies parts are reported also in [34, 35, 37, 38, 40]. The authors of [37] unambiguously ascribe this low-frequency part to solid-state diffusion of

lithium. However, for the conditions of plane semi-infinitive diffusion this slope is known to be 1 (tan $\pi/4$), and this very value is reported in [30–32, 41].

The parts of impedance spectra corresponding to the highest frequencies contain certain segments with positive reactive component. This points to inductive character of the impedance. The nature of this inductance is unclear. In [31] the presence of inductive component was explained by some external factor like an entangled electric wire. The authors of [37] reported about well-pronounced inductive loop at impedance spectra measured at rather negative potentials. According to these authors the main origin of the inductive phenomenon on the impedance spectra is the instability of the solid electrolyte interphase (SEI) on the Si particle surface.

The impedance data have been fitted with the equivalent circuit shown in Fig. 5.

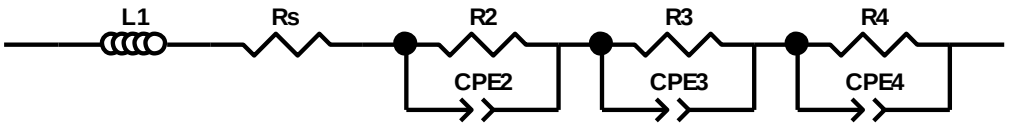

Figure 5. Equivalent circuit of the electrodes; explanations in text.

The equivalent circuit comprises five units connected in series. The first unit is inductance L1, the second one is the resistance Rs including all ohmic resistances in the system other than the resistances of electrical double layers and diffusion regions. Three other units are parallel combinations of a resistances R2, R3 and R4 with constant-phase elements (CPEs). This very equivalent circuit but without inductance was used in [30]. Noteworthy is that a variety of equivalent circuits for silicon-based electrodes can be found in the literature. For instance, the same equivalent circuit as in Fig. 5, but with Warburg element instead of inductance was used in [41]. Close equivalent circuit is cited in [40] but in this case one of CPEs was not shunted by resistance. References [38–40] report on more simplified equivalent circuits, whereas [37] presents much more complex, and therefore, less reliable equivalent circuit for silicon-based electrodes.

Usually, series resistance Rs is identified with an electrolyte resistance. In the present work, this is far from being the case. Indeed, the electrolyte resistance does not change in the course of storage, whereas Rs notably rises but non-monotonously during storage (Fig. 6).

Non-monotonous change of Rs as well as non-monotonous change of corrosion current point to dynamic character of steady-state, specifically continuous formation and destruction of SEI.

Each CPE is known to be characterized by a power *n*. For CPE2, *n* was close to 1 and didn't vary in the course of storage. Therefore, with certain approximation CPE2 could be identified as double layer capacity at the interface between Si and SEI. Absolute values of this capacity at the very beginning of the experiment, and after 456, 768, 1080, and 1512 hours amounted to 90, 84, 85, 84, and 64 $\mu F\ cm^{-2}$, that seems to be rather realistic. It must be stressed, that all values of the equivalent circuit elements presented in the paper refer to visible (geometric) surface area of the electrode. With due account of porosity (cracks etc.) of active layers, true surface area covered by SEI could be estimated as 10–30 cm^2 per 1 cm^2 of visible surface area. This estimation is based on SEM images presented in

Ref. [28]. Therefore, true double layer capacity must be 3–9 μF cm^{-2}. If so, R2 may be identified as resistance of charge transfer at the interface. R2 values at the abovementioned moments were 7.9, 4.9, 6.7, 10.6, and 11.2 Ohm.cm^2, that corresponds to the exchange current density of 3.1, 5.1, 3.7, 2.4, and 2.2 mA cm^{-2}. These quantities are realistic as well.

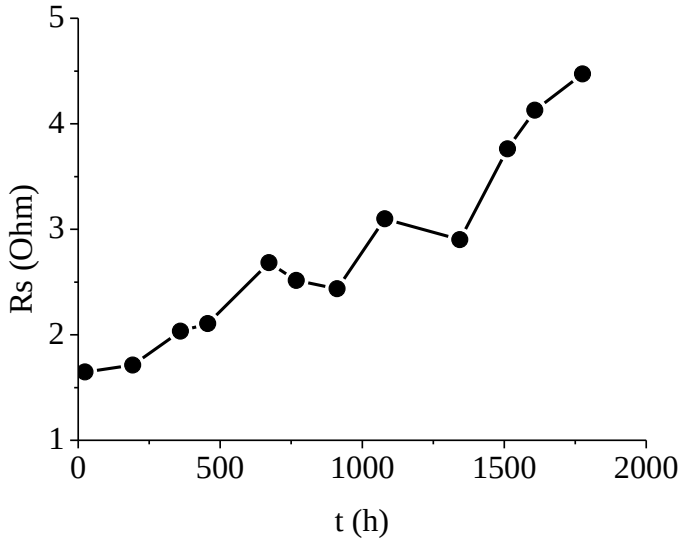

Figure 6. Evolution of Rs during storage

The parallel combination of CPE3 and R3 can be related to the charge transfer through the SEI. The power *n* in CPE3 varies but insignificantly in the course of storage, falling in the 0.65–0.75 range. At the same time, R3 corresponding to SEI resistance varies noticeably and chaotically.

Fig. 7 demonstrates the comparison of R2 and R3 variation at storage. One can see certain synchronism in behavior of both resistances, that confirms dynamic character of stationary state.

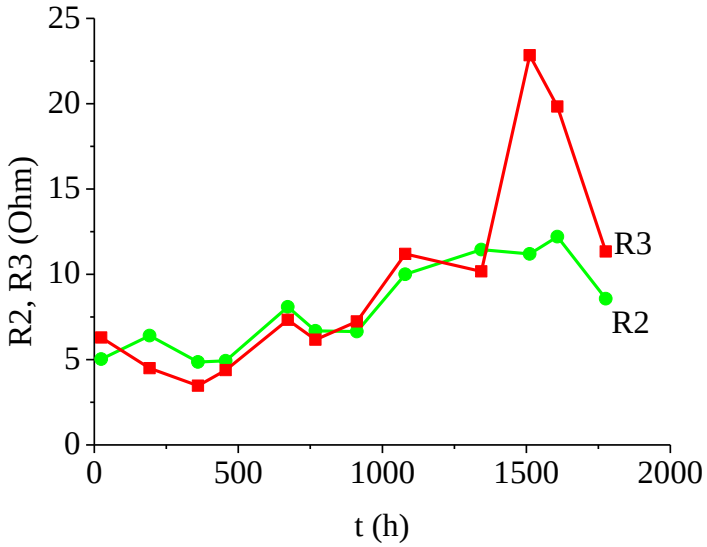

Figure 7. Variation of R2 and R3 at storage.

4. CONCLUSIONS

In this work, the behavior of silicon-based electrode during storage at open circuit conditions was studied for the first time. Noticeable self-discharge is shown to take place during o.c.p. storage. It was happened that self-discharge current varies in non-monotonous manner upon storage that suggests a dynamical character of SEI formation and destruction. This conclusion is confirmed also by results of EIS measurements. Indeed, certain elements of equivalent circuit chaotically vary upon storage.

ACKNOWLEDGEMENT
The present work is financially supported by the Ministry of Education and Science of the Russian Federation (the Agreement No. 14.604.21.0126 of August 26, 2014. Unique identifier of applied scientific researches RFMEFI60414X0126).

References

1. M. Broussely, S. Herreyre, P. Biensan, P. Kasztejna, P. Nechev, R. Stanievicz, *J. Power Sources*, 97/98 (2001) 13–21.
2. I. Bloom, B. W. Cole, J. J. Sohn, S. A. Jones, E. G. Polzin, V. S. Battaglia, G. L. Henriksen, C. Motloch, R. Richardson, T. Unkelhaeuser, D. Ingersoll, H. L. Case, *J. Power Sources*, 101 (2001) 238–247.
3. R. B. Wright, C. G. Motloch, J. R. Belt, J. P. Christophersen, C. D. Ho, R. A. Richardson, I. Bloom, S. A. Jones, V. S. Battaglia, G. L. Henriksen, T. Unkelhaeuser, D. Ingersoll, H. L. Case, S. A. Rogers, R. A. Sutula, *J. Power Sources*, 110 (2002) 445–470.
4. R.P. Ramasamy, R.E. White, B.N. Popov, *J. Power Sources*, 141 (2005) 298–306.
5. Zhang Qi, R. E. White, *J. Power Sources*. 173 (2007) 990–997.
6. G. Sarre, Ph. Blanchard, M. Broussely, *J. Power Sources*, 127 (2004) 65–71.
7. M. Kassem, J. Bernard, R. Revel, S. Pélissier, F. Duclaud, C. Delacourt, *J. Power Sources*, 208 (2012) 296–305.
8. I. Bloom, L. K. Walker, J. K. Basco, D. P. Abraham, J. P. Christophersen, C. D. Ho, *J. Power Sources*, 195 (2010) 877–882.
9. J. Belt, V. Utgikar, I. Bloom, *J. Power Sources*, 196 (2011) 10213–10221.
10. M. Ecker, J. B. Gerschler, J. Vogel, S. Käbitz, F. Hust, Ph. Dechent, D. U. Sauer, *J. Power Sources*, 215 (2012) 248–257.
11. S. Käbitz, J. B. Gerschler, M. Ecker, Y. Yurdagel, B. Emmermacher, D. André, T. Mitsch, D. U. Sauer, *J. Power Sources*, 239 (2013) 572–583.
12. M. Ecker, N. Nieto, S. Käbitz, J. Schmalstieg, H. Blanke, A. Warnecke, D. U. Sauer, *J. Power Sources*, 248 (2014) 839–851.
13. R. Yazami, Y.F. Reynier., *Electrochim. Acta*, 47 (2002) 1217–1223.
14. Ch. Wang, Xiang-wu Zhang, A.J. Appleby, X. Chen, F.E. Little, *J. Power Sources*, 112 (2002) 98–104.
15. M. D. Levi, C. Wang and D. Aurbach., *J. Electrochem. Soc.*, 151 (2004) A781–A790.
16. R.P. Ramasamy, Jong-Won Lee, B.N. Popov, *J. Power Sources*, 166 (2007) 266–272.
17. D. Ostrovskii, F. Ronci, B. Scrosati, P. Jacobsson., *J. Power Sources*, 94 (2001) 183–188.
18. Sun Hee Choi, Joosun Kim, Young Soo Yoon., *J. Power Sources*, 138 (2004) 283–287.
19. B. Key, R. Bhattacharyya, M. Morcrette, V. Seznéc, J.-M. Tarascon, C. P. Grey, *J. Am. Chem. Soc.*, 131 (2009), 9239–9249.

20. Sh. Komaba, K. Shimomura, N. Yabuuchi, T. Ozeki, H. Yui, K. Konno, *J. Phys. Chem. C,* 115 (2011) 13487–13495.
21. Yu. E. Roginskaya, T. L. Kulova, A. M. Skundin, M. A. Bruk, A. V. Klochikhina, N. V. Kozlova, V. A. Kal'nov, and B. A. Loginov, *J. Physical Chemistry A*, 82 (2008) 1655−1662.
22. Yu.E.Roginskaya, T.L.Kulova, A.M.Skundin, M.A.Bruk, E.N.Zhikharev, V.A.Kal'nov, and V.B.Loginov., *Russian J. Electrochemistry*, 44 (2008) 1197−1203.
23. Chang-Mook Hwang, Jong-Wan Park., *J. Power Sources,* 196 (2011) 6772– 6780.
24. Jae-Bum Kim, Sung-Hwan Lim, and Sung-Man Leez., *J. Electrochem. Soc*., 153 (2006) A455−A458.
25. A. E. Berdnikov, V. N. Gerashchenko, V. N. Gusev, T. L. Kulova, A. V. Metlitskaya, A. A. Mironenko, A. S. Rudyi, and A. M. Skundin., *Technical Physics Letters*, 39 (2013) 350–352.
26. M.T. Demirkan, L. Trahey, T. Karabacak., *J. Power Sources,* 273 (2015) 52–61.
27. T. L. Kulova, A. M. Skundin, V. N. Andreev, D. Yu. Gryzlov, A. A. Mironenko, A. S. Rudyi, V. N. Gusev, and V. V. Naumov., *Russian Journal of Electrochemistry,* 51 (2015) 1157–1161.
28. T.L.Kulova, A.A.Mironenko, A.M.Skundin, A.S.Rudy, V.V.Naumov, D.E.Pukhov., *Int. J. Electrochem. Sci*., 11 (2016) 1370–1381.
29. T. L. Kulova, Yu. V. Pleskov, A. M. Skundin, E. I. Terukov, and O. I. Kon'kov., *Russian Journal of Electrochemistry*, 42 (2006) 708–714.
30. T. L. Kulova, A. M. Skundin, Yu. V. Pleskov, E. I. Terukov, O. I. Kon'kov, *J. Electroanalyt. Chem.*, 600 (2007) 217−225.
31. Y.-M. Kang, J.-Y. Go, S.-M. Lee, W.-U. Choi, *Electrochem. Comm.,* 9 (2007) 1276–1281.
32. T. Jiang, Sh. Zhang, X. Qiu, W. Zhu, L. Chen, *Electrochem. Comm.,* 9 (2007) 930–934.
33. Y. H. Xu, G. P. Yin, Y. L. Ma, P. J. Zuo, X. P. Cheng, *J. Power Sources,* 195 (2010) 2069–2073.
34. G.-B. Han, M.-H. Ryou, K. Y. Cho, Y. M. Lee, J.-K. Park, *J. Power Sources,* 195 (2010) 3709–3714.
35. R. Lv, J. Yang, J. Wang, Y. NuLi, *J. Power Sources,* 196 (2011) 3868–3873.
36. H. Usui, Y. Yamamoto, K. Yoshiyama, T. Itoh, H. Sakaguchi, *J. Power Sources,* 196 (2011) 3911–3915.
37. E. Radvanyi, K. Van Havenbergh, W. Porcher, S. Jouanneau, J.-S. Bridel, S. Put, S. Franger, *Electrochim. Acta,* 137 (2014) 751–757.
38. J-S. Bridel, T. Azaïs, M. Morcrette, J-M. Tarascon, and D. Larcher., *J. Electrochem. Soc.*, 158 (2011) A750–A759.
39. S.S. Zhang, K. Xu, T.R. Jow., *Electrochim. Acta,* 51 (2006) 1636–1640.
40. Pengjian Zuo, Geping Yin, Yulin Ma., *Electrochim. Acta,* 52 (2007) 4878–4883.
41. Juchen Guo, Ann Sun, Xilin Chen, Chunsheng Wang, Ayyakkannu Manivannan., *Electrochim. Acta,* 56 (2011) 3981–3987.